Performance Analysis of Uplink NOMA-IoT Networks with Space-Time Line Code

Jaewon Bae, Ki-Hun Lee[†], Jong Min Kim, Bang Chul Jung[†], and Jingon Joung[‡]

Korea Science Academy of KAIST, Busan, South Korea

[†]Department of Electronics Engineering, Chungnam National University, Daejeon, South Korea

[‡]School of Electrical and Electronics Engineering, Chung-Ang University, Seoul, South Korea

Email: jwje0219@gmail.com, kihun.h.lee@cnu.ac.kr, franzkim@gmail.com, bcjung@cnu.ac.kr, jgjoung@cau.ac.kr

Abstract—In this paper, we investigate the performance of uplink non-orthogonal multiple access (NOMA) systems for internet-of-things (IoT) applications, which exploits a space-time line code (STLC) and a binary phase shift keying (BPSK) modulation at each sensor (transmitter). A single transmit antenna is assumed to be equipped at the sensor and two receive antennas are assumed to be equipped at a fusion center (FC). The STLC enables the FC to decode the transmitted symbols from multiple sensors without channel state information (CSI) of each sensor. In particular, we mathematically analyze the symbol error rate (SER) of the super-imposed symbol received at the FC and obtain the diversity order of the uplink NOMA-IoT network. We also propose a phase steering (PS)-based STLC technique to improve the SER performance, in which certain sensors rotate its constellation. The proposed PS-STLC technique significantly outperforms the conventional STLC scheme in the uplink NOMA-IoT network.

Index Terms—Non-orthogonal multiple access (NOMA), uplink IoT network, space-time line code (STLC), diversity order, symbol error rate (SER), phase steering.

I. INTRODUCTION

Non-orthogonal multiple access (NOMA) is one of the most promising techniques being considered as a multiple access technique in the fifth generation (5G) cellular networks due to its high spectral efficiency [1]. The basic idea of NOMA is to share the time, frequency, or power resource for two or more users by allowing an inter-user interference (IUI) [2]. By sharing the radio resources, it is expected that the NOMA satisfies the requirements of the 5G network such as increased connection density and reduced latency [3]. In [4], the authors analyzed the symbol error rate (SER) performance of the NOMA systems when a receiver detects the transmitted signals with a successive interference cancellation (SIC) technique. The SIC-based detector is typically used for the downlink NOMA and it has been shown to be suboptimal for the uplink NOMA [5], [6].

Most studies of the NOMA uplink communications assume that channel state information (CSI) is available at a receiver (CSIR). However, the enormous orthogonal pilot signals are required to estimate the CSI from each sensor to a fusion center (FC) in internet-of-things (IoT) networks, which significantly reduces the efficiency of uplink resource usage. Meanwhile, a space-time line code (STLC) technique, proposed in [7], can achieve full diversity gain when the CSI is available only at the transmitter (CSIT), i.e., the sensors. In this case, two-orthogonal-broadcast pilot signals are sufficient for all sensors to estimate the CSI under the assumption that the uplink-and-downlink channels are symmetric in time division duplex (TDD) systems. Many studies have been performed about STLC-based communication systems. In [8], he considered a massive multiple-input multiple-output system with STLC, also, in [9], proposed an STLC-based two-way relay system to improve the energy efficiency. In [10], they proposed a zero-forcing (ZF)-based multiuser STLC system. In particular, in [11], they proposed a machine learning-based blind decoding method for STLC. This technique allows the receiver to obtain the effective channel gain of the STLC transmitter in a blind manner. In this paper, we propose to apply STLC for the uplink NOMA-IoT networks. We first analyze the SER of the uplink NOMA-IoT with two STLC sensors and show that the significant IUIs hinder STLC from achieving the full diversity gain. To resolve this problem, we propose a novel phase steering-based STLC (PS-STLC) technique and analyze the SER. The optimal phase steering angle to minimize the SER is also derived. It is shown that the proposed PS-STLC significantly outperforms the conventional STLC in the uplink NOMA-IoT networks. In particular, the proposed PS-STLC achieves the optimal diversity gain even though an arbitrary phase steering angle is chosen.

The remainder of this paper is organized as follows. In Section II, we introduce the system model we consider in this paper. In Section III, we analyze the SER performance of uplink NOMA-IoT network with both the conventional STLC and the proposed PS-STLC techniques. In Section IV, we validate the analytical results via extensive simulation results. Conclusion is drawn in Section V.

II. SYSTEM MODEL

We consider an uplink NOMA system consisting of a single FC with two antennas and two sensors with a single antenna as shown in Fig. 1. It is assumed that every sensor knows the CSI from itself to the FC through a pilot signal transmitted by the FC, but the FC does not have the CSI of sensors at all. The transmit signals of each sensor are modulated by the binary phase-shift keying (BPSK) modulation. Each sensor encodes the BPSK symbols to two STLC [7] signals by using its CSI, and transmits them via two symbol times. The CSI is assumed not to change during the two symbol times. We propose a
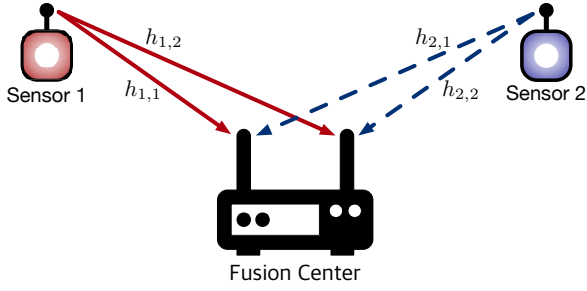
Fig. 1. System model of two-sensor uplink NOMA-IoT networks

novel PS-STLC in this paper. Then, the STLC encoded signals of the i th sensor are given by

$$s_{i,1} = \frac{h_{i,1}^*\sqrt{P_i}x_{i,1}e^{j\theta_i} + h_{i,2}^*\sqrt{P_i}x_{i,2}^*e^{-j\theta_i}}{\sqrt{\gamma_i}},$$

$$s_{i,2} = \frac{h_{i,2}^*\sqrt{P_i}x_{i,1}^*e^{-j\theta_i} - h_{i,1}^*\sqrt{P_i}x_{i,2}e^{j\theta_i}}{\sqrt{\gamma_i}}, \qquad (1)$$

where $x_{i,t}$ and $s_{i,t}$ denote the BPSK modulated symbol of the $i(i \in \{1,2\})$th sensor in the $t(t \in \{1,2\})$th symbol time and the STLC signal of the ith sensor which is transmitted at tth symbol time, respectively. In addition, P_i and θ_i denote the transmit power and the steering angle of the ith sensor, respectively. The wireless channel between ith sensor and mth antenna of the FC is denoted as $h_{i,m}$, and all channels are assumed to follow an identically independently distributed (i.i.d) complex Gaussian distribution with zero mean and variance of σ_i^2, i.e., $h_{i,m} \sim \mathcal{CN}(0, \sigma_i^2)$. In order to normalize the transmitted signals, the STLC signals are divided by wireless channel gain represented by $\sqrt{\gamma_i} = \|\mathbf{h}_i\|$ where $\mathbf{h} = [h_{i,1} \ h_{i,2}]^T$.

All sensors transmit the STLC signals to the FC simultaneously during two symbol times and the FC receives the superposed signals from multiple sensors. Then, the received signal at the mth antenna of the FC at t-th symbol time is given by

$$\begin{bmatrix} y_{1,1} & y_{1,2} \\ y_{2,1} & y_{2,2} \end{bmatrix} = \sum_{i=1}^{2} \mathbf{h}_i \begin{bmatrix} s_{i,1} & s_{i,2} \end{bmatrix} + \begin{bmatrix} w_{1,1} & w_{1,2} \\ w_{2,1} & w_{2,2} \end{bmatrix}, \qquad (2)$$

where $w_{m,t}$ denotes the additive Gaussian noise (AWGN) following zero mean and variance of N_0, i.e., $w_{m,t} \sim \mathcal{CN}(0, N_0)$. The FC performs a linear combination using four received signals (Eq. (2)) to decode the transmitted signals of each sensor as follows.

$$r_1 = y_{1,1} + y_{2,2}^* = \sum_{i=1}^{2} \sqrt{\gamma_i}\sqrt{P_i}x_{i,1}e^{j\theta_i} + w_{1,1} + w_{2,2}^*,$$
$$r_2 = y_{2,1}^* - y_{1,2} = \sum_{i=1}^{2} \sqrt{\gamma_i}\sqrt{P_i}x_{i,2}e^{j\theta_i} + w_{2,1}^* - w_{1,2}. \qquad (3)$$

Interestingly, the t-th BPSK symbol of each sensor is superimposed on the $k(k \in \{1,2\})$-th result. Here, we define the sum of the AWGN in each r_k as n_k, i.e., $n_k \sim \mathcal{CN}(0, 2N_0)$.
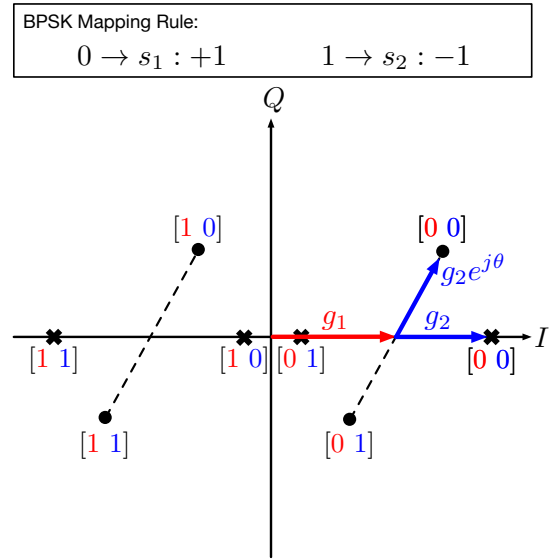

Fig. 2. Received signal model of BPSK symbols from two users at the BS of both conventional and PS STLC in uplink NOMA system

Finally, the FC detects each transmitted symbol from the three sensors using the joint maximum likelihood (ML) detector as follows:

$$[\hat{x}_{1,k}, \hat{x}_{2,k}] = \arg\min_{x_{i,k} \in \mathcal{X}} \|\tilde{r}_k - \sum_{i=1}^{2} g_i x_{i,k}e^{j\theta_i}\|^2, \qquad (4)$$

where $\mathcal{X} \triangleq \{s_1, s_2\} = \{+1, -1\}$ and $g_i \triangleq \sqrt{\gamma_i P_i}$.

III. THEORETICAL ANALYSIS

In this section, we consider the two bits transmitted by two sensors simultaneously as a single symbol at the FC, and analyze the SER performance. Let define the received signal-to-noise ratio (SNR) of each sensor at the FC as $\rho_i = P_i\sigma_i^2/N_0$ ($i \in \{1,2\}$). Furthermore, we define some random variables, X_i, Z and N as: $X_i := g_i$, $Z := |n|$, and $N := \text{Re}\{n\}$, and then the probability density functions (PDFs) of the random variables are given by:

$$f_{X_i}(x_i) = \frac{2x_i^3}{P_i^2\sigma_i^4}\exp\left(-\frac{x_i^2}{P_i\sigma_i^2}\right) \qquad (x_i \geq 0),$$

$$f_N(n) = \frac{1}{\sqrt{2\pi N_0}}\exp\left(-\frac{n^2}{2N_0}\right) \qquad (n \in \mathbb{R}),$$

$$f_Z(z) = \frac{z}{N_0}\exp\left(-\frac{z^2}{2N_0}\right) \qquad (z \in \mathbb{R}). \qquad (5)$$

A. SER of uplink NOMA with the conventional STLC

Fig. 2 shows the superimposed BPSK symbols from two sensors at the FC in uplink NOMA with conventional STLC and PS-STLC. The conditional probabilities of SER when applying conventional STLC are given by

$$\Pr(\mathcal{E}|00) = \Pr(\mathcal{E}|11) = \Pr(N > Y),$$
$$\Pr(\mathcal{E}|01) = \Pr(\mathcal{E}|10) = \Pr(N > V) + \Pr(N > Y), \qquad (6)$$

where $V := |X_1 - X_2|$ and $Y := \min(X_1, X_2)$. Using (6), the SER of the uplink NOMA system with the conventional STLC is given by

$$\Pr(\mathcal{E}) = \frac{1}{2}\Pr(N > V) + \Pr(N > Y). \quad (7)$$

The PDFs of the random variables V and Y are given by

$$f_V(v) = \frac{e^{-v^2}}{32}\left(2v(v^4 - 4v^2 + 15) - \sqrt{2\pi}e^{v^2/2}g(v)Q(v)\right),$$

$$f_Y(y) = \sum_{i=1}^{2} f_{X_i}(y)(1 - F_{X_i}(y)), \quad (8)$$

where $g(v) = v^6 - 3v^4 + 9v^2 - 15$ and $Q(v) := \frac{1}{\sqrt{2\pi}}\int_v^\infty e^{-t^2/2}dt$, and $F_{X_i}(y)$ is the cumulative density function (CDF) of the random variable X_i. Each term in (7) can be calculated by follows:

$$\Pr(N > V) = \int_0^\infty \left(\int_v^\infty f_N(t)dt\right)f_V(v)dw,$$

$$\Pr(N > Y) = \int_0^\infty \left(\int_y^\infty f_N(t)dt\right)f_Y(y)dy. \quad (9)$$

Then, the exact SER can drive by

$$\Pr(\mathcal{E}) = \frac{3}{4} - \frac{48 + 385N_0 + 933N_0^2}{64(1 + 2N_0)^{\frac{5}{2}}} + \frac{1}{64}(a + b + c), \quad (10)$$

where

$$a = \frac{15N_0^{1/2}\left((1 + 2N_0)^{1/2} - N_0^{1/2}\right)}{(1 + N_0)(1 + 2N_0)^{1/2}},$$

$$b = \frac{2N_0^{3/2}\left[2(1+2N_0)^{1/2} + N_0^{1/2}\left\{-3 - 5N_0 + 4(1+2N_0)^{1/2}\right\}\right]}{(1+N_0)^2(1+2N_0)^{3/2}},$$

$$c = \frac{N_0^{5/2}\left[8(1+2N_0)^{1/2} + N_0^{1/2}\left\{N_0^{1/2}\left(32(1+2N_0)^{1/2} + \delta\right) - 15\right\}\right]}{(1+N_0)^3(1+2N_0)^{5/2}},$$

$$\delta = N_0^{1/2}(-50 - 43N_0 + 32N_0^{1/2}(1 + 2N_0)^{1/2}).$$

Applying Taylor series expansion to (10), the SER performance of the uplink NOMA with the conventional STLC can be approximated in high SNR regime as follow:

$$\Pr(\mathcal{E}) \approx \frac{1}{2}P(N > V) \approx \frac{15}{64}\rho^{-\frac{1}{2}}. \quad (11)$$

B. Optimal steering angle of PS-STLC

Without loss of generality, we fix θ_1 to zero and assume that $\theta_2 = \theta \in (0, \frac{\pi}{2}]$[rad]. Since two random variables, X_1 and X_2 are independent, the SER performance of the uplink NOMA with PS-STLC is given by

$$\Pr(\mathcal{E}) = \int_0^\infty\int_0^\infty \Pr(\mathcal{E}|X_i = x_i)f_{X_1}(x_1)f_{X_2}(x_2)dx_1dx_2, \quad (12)$$

where

$$\Pr(\mathcal{E}|X_i = x_i) = 1 - \left\{\frac{1}{4}\left(1 + \mathrm{erf}\left(\frac{g_1}{\sqrt{2N_0}}\right) + \mathrm{erf}\left(\frac{g_2}{\sqrt{2N_0}}\right)\right) + \frac{\Pr(S)}{2}\right\}. \quad (13)$$

The lower bound of the SER is derived by the upper bound of the probability of successful detection, $\Pr(S)$. Using the property of complex Gaussian distribution and joint ML detection, we find the upper bound of $\Pr(S)$ is given by

$$\Pr(S) \leq \Pr\{\mathrm{Re}(n) \in (-g_1, g_1), \mathrm{Im}(n) \in (0, g_2)\}. \quad (14)$$

Since both $\mathrm{Re}(n)$ and $\mathrm{Im}(n)$ follow Gaussian distribution, the upper bound is calculated simply. Using (12) and (14), the bounds of conditional probability are given by

$$\Pr(\mathcal{E}|X_i = x_i) \geq 1 - \left(1 - Q\left(\frac{g_1}{\sqrt{N_0}}\right)\right)\left(1 - Q\left(\frac{g_2}{\sqrt{N_0}}\right)\right). \quad (15)$$

Therefore, the lower bound of SER is given by

$$1 - \frac{\left(1 + \frac{\sqrt{P_1}\sigma_1(P_1\sigma_1^2 + 3N_0)}{(P_1\sigma_1^2 + 2N_0)^{\frac{3}{2}}}\right)\left(1 + \frac{\sqrt{P_2}\sigma_2(P_2\sigma_2^2 + 3N_0)}{(P_2\sigma_2^2 + 2N_0)^{\frac{3}{2}}}\right)}{4}. \quad (16)$$

Note that (16) is exactly the same as the exact SER formula of PS-STLC with $\theta = \pi/2$. As a result, $\pi/2$ rad is the optimal phase of PS-STLC for the uplink NOMA with two sensors.

C. SER of PS-STLC when $\theta = \pi/2$

When the steering angle is equal to $\pi/2$, i.e., $\theta = \pi/2$, two terms $g_1e^{j\theta_1}$ and $g_2e^{j\theta_2}$ are perpendicular to each other. Thus, the four received signals in Fig. 2 form a rectangle as a special case of a parallelogram. The conditional probability of SER applying PS-STLC with $\theta = \pi/2$ is exactly the same as (15). Hence, the exact SER of PS-STLC with optimal θ is equal to (16). Applying Taylor series expansion to (16), the SER of PS-STLC with the optimal phase in the uplink NOMA-IoT network is approximated as

$$\Pr(\mathcal{E}) \approx \frac{3}{4}(\rho_1^{-2} + \rho_2^{-2}). \quad (17)$$

D. Upper bound of SER of PS-STLC with arbitrary steering angle

As noted before, the lower bound of SER of the uplink NOMA-IoT network with PS-STLC is given by (16). We now derive the upper bound of SER of the uplink NOMA-IoT network with PS-STLC for arbitrary steering angle. The conditional probabilities of SER for the eight possible received signals are upper bounded by

$$\Pr(\mathcal{E}|11) = \Pr(\mathcal{E}|00) \leq \frac{\Pr(Z > \delta_1)}{2},$$

$$\Pr(\mathcal{E}|10) = \Pr(\mathcal{E}|01) \leq \frac{\Pr(Z > \delta_1) + \Pr(Z > \delta_2)}{2}, \quad (18)$$

where

$$\delta_1 = \min(g_1, g_2), \quad \delta_2 = \sqrt{(g_2\sin\theta)^2 + (g_1 - g_2\cos\theta)^2}.$$

Each upper bound is also upper bounded as follow:

$$\Pr(N > \delta_1) \leq \Pr(Z > g_1) + \Pr(Z > g_2),$$

$$\Pr(Z > \delta_2) \leq \Pr\left(\frac{|g_2\sin\theta| + |g_1 - g_2\sin\theta|}{\sqrt{2}}\right), \quad (19)$$

where the length of a right triangle's hypotenuse is equal to or greater than $1/\sqrt{2}$ times the sum of the two sides. We obtain the upper bound of SER by the inequality which is given by

$$\Pr(Z > x + y) \le \exp(-x^2)\exp(-y^2) \text{ for } x, y > 0.$$

The term $\int_0^\infty \exp\left(-\frac{(x-y)^2}{4N_0}\right) f_{X_1}(x_1) dx_1$ has an upper bound as

$$\frac{4e^{-\frac{y^2}{4N_0}}(y^2 P_1\sigma_1^2 + 4N_0(P_1\sigma_1^2 + 4N_0))N_0}{(P_1\sigma_1^2 + 4N_0)^3} \tag{20}$$
$$+ \frac{4\sqrt{\pi P_1\sigma_1^2}e^{-\frac{y^2}{P_1\sigma_1^2+4N_0}}y(y^2 + 6N_0(P_1\sigma_1^2 + 4N_0))N_0^{\frac{1}{2}}}{(P_1\sigma_1^2 + 4N_0)^{\frac{7}{2}}}.$$

Using (12) and (18) to (20), we obtain the upper bound of SER which is given by

$$\Pr(\mathcal{E}) \le \frac{1}{2}\left(\int_0^\infty e^{-\frac{x^2}{2N_0}} f_{X_1}(x)dx + \int_0^\infty e^{-\frac{x^2}{2N_0}} f_{X_2}(x_2)dx\right)$$
$$+ \frac{1}{4}\int_0^\infty\int_0^\infty e^{-\frac{(x_2\sin\theta)^2+(x_1-x_2\cos\theta)^2}{4N_0}} f_{X_1}(x_1)f_{X_2}(x_2)dx_1 dx_2$$
$$= \frac{2N_0^2}{(P_1\sigma_1^2+2N_0)^2} + \frac{2N_0^2}{(P_2\sigma_2^2+2N_0)}$$
$$+ \frac{64(2P_1\sigma_1^2 P_2\sigma_2^2\beta^2 + (P_1\sigma_1^2+4N_0)(P_2\sigma_2^2+4N_0))N_0^4}{(P_1\sigma_1^2+4N_0)^3(P_2\sigma_2^2+4N_0)^3}$$
$$+ \frac{48\pi\beta\sqrt{P_1\sigma_1^2 P_2\sigma_2^2}(48N_0^2+P_1\sigma_1^2 P_2\sigma_2^2(5\beta^2+3\alpha^2)+12N_0(P_1\sigma_1^2+P_2\sigma_2^2))N_0^4}{(16N_0^2+4N_0(P_1\sigma_1^2+P_2\sigma_2^2)+\alpha^2 P_1\sigma_1^2 P_2\sigma_2^2)^{\frac{7}{2}}}, \tag{21}$$

where $\alpha = \sin\theta$ and $\beta = \cos\theta$. Applying Taylor series expansion to (21), the upper bound of SER is approximated in high SNR regime as

$$\Pr(\mathcal{E}) \lessapprox 2\rho_1^{-2} + 2\rho_2^{-2} - 8\rho_1^{-3} + 8\rho_2^{-3} \tag{22}$$
$$+ 16\left(4(2\beta^2+1) + \frac{3\pi\beta(5\beta^2+3\alpha^2)}{\alpha^7}\right)\rho_1^{-2}\rho_2^{-2}.$$

The coefficient of N_0^4 is large when the steering angle is small, so we express the upper bound up to order of N_0^4. Since the optimal phase is $\pi/2$ rad, by (17) and (22), the SER of the uplink PS-STLC NOMA for any steering angle is bounded in high SNR regime as

$$\frac{3}{4}(\rho_1^{-2} + \rho_2^{-2}) \le P(\mathcal{E}) \le 2(\rho_1^{-2} + \rho_2^{-2}). \tag{23}$$

E. Diversity order of the conventional STLC and PS-STLC

The diversity order is defined as:

$$\eta_k = -\lim_{\rho_k \to \infty} \frac{\log\Pr(\mathcal{E})}{\log\rho},$$

which is used to figure out the behavior of error probability in the high SNR regime [12]. By the definition of the diversity order, (11) shows that the diversity order of the conventional STLC in the uplink NOMA-IoT network is equal to $1/2$. The conventional STLC cannot achieve the full diversity gain in the uplink NOMA systems. We also obtain that the diversity order of PS-STLC with any steering angle in the uplink NOMA-IoT network is equal to 2, as shown in (22), which is the optimal achievable diversity order in our system model. Therefore, PS-STLC achieves the optimal diversity order.
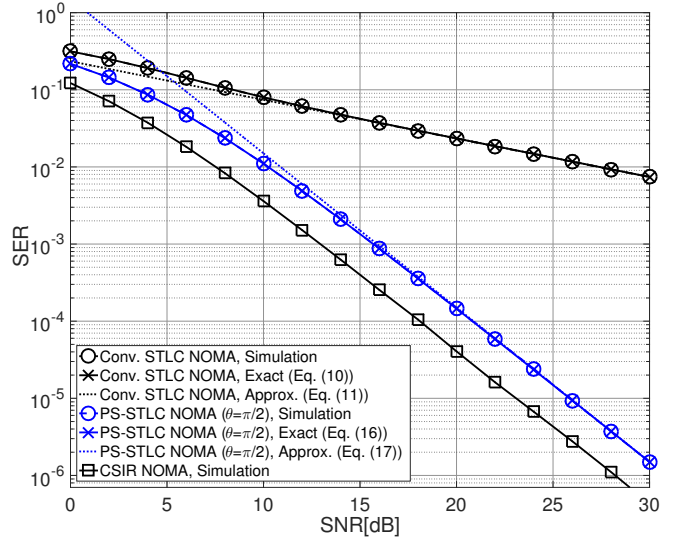

Fig. 3. SER performance of the uplink NOMA-IoT network with both conventional STLC and the proposed PS-STLC techniques when the optimal steering angle is applied ($\theta = \pi/2$).

IV. SIMULATION RESULTS

In this section, we validate the theoretical analysis provided in Section III via extensive computer simulations. Fig. 3 shows the SER performance of the uplink NOMA-IoT network with the conventional STLC and the proposed PS-STLC techniques for varying the SNR values. We assume that two sensors have the same transmit power for simplicity, i.e., $P_1 = P_2$. In Fig. 3, we assume that $\sigma_1 = \sigma_2$ and thus $\rho_1 = \rho_2$. As a benchmark technique, the SER performance of the conventional NOMA system with CSI at the receiver (CSIR) is also compared in Fig. 3. The SER performance of the uplink NOMA-IoT network with the conventional STLC technique is much worse than the SER of the conventional NOMA-IoT network with CSIR. Note that the slopes of two schemes are different each other. The closed-form exact SER of the conventional STLC in (10) is perfectly matched with the simulation result and the approximation in (11) also matches well with the simulation results as SNR increases. The proposed PS-STLC technique significantly improves the SER performance compared with the conventional STLC technique. In Fig. 3, we apply the optimal steering angle for the PS-STLC technique, i.e., $\theta = \pi/2$. The closed-form exact SER of the PS-STLC in (16) is also perfectly matched with the simulation result and the approximation in (17) becomes matched well with the simulation as SNR increases. It is worth noting that the slope of SER of the PS-STLC is the same as the NOMA-IoT network with CSIR, which implies the PS-STLC achieves the full diversity gain.

Fig. 4 shows the SER performance of the proposed PS-STLC technique with various steering angles in the uplink NOMA-IoT network according to SNR values. Somewhat interestingly, the SER performances with various steering angles become similar to that with the optimal steering angle
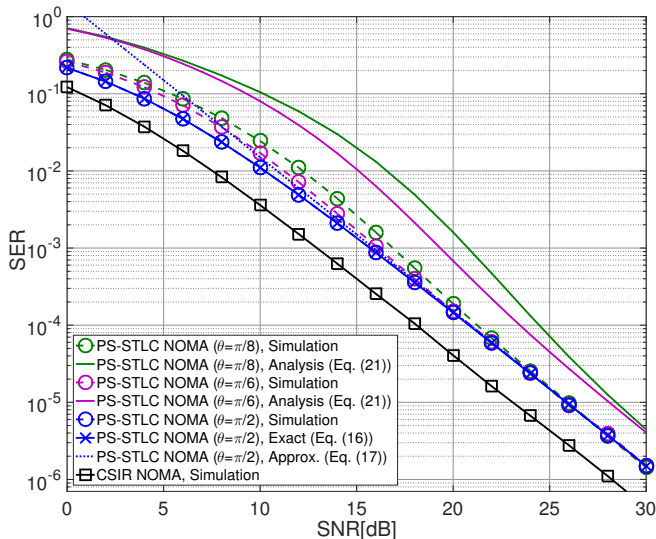
Fig. 4. SER performance of the proposed PS-STLC with various steering angles in the uplink NOMA-IoT network for varying SNR values.

for high SNR regime, which supports that the optimal diversity gain can be achieved with any steering angle as long as $\theta \neq 0$ as noted in Section III. For all SNR values, the optimal steering angle is equal to $\pi/2$ for minimizing SER. The PS-STLC technique significantly outperforms the conventional STLC with any steering angle, comparing with Fig. 3. The upper bound on the SER performance of the PS-STLC technique in (21) has about 2dB gap from the simulation result for high SNR regime. The upper bound in (21) becomes tight as SNR increases even though it has a certain constant gap in dB scale for SNR values.

V. CONCLUSION

In this paper, we mathematically characterized the symbol error rate (SER) performance of the uplink non-orthogonal multiple access-based internet-of-things (NOMA-IoT) network when the space-time line code (STLC) is adopted at each sensor for exploiting the spatial diversity. We obtained the exact SER performance of the conventional STLC applied to the uplink NOMA-IoT network. We found that the SER performance becomes deteriorated if we apply the conventional STLC technique for the uplink NOMA-IoT network. Thus, we proposed a novel phase-steering based STLC (PS-STLC) technique for the network and analyzed its SER performance. The PS-STLC technique significantly outperforms the conventional STLC technique for all signal-to-noise ratio (SNR) values. It was shown that the optimal steering angle is equal to $\theta = \pi/2$

for minimizing the SER and the optimal diversity gain can be achieved by the proposed PS-STLC with any steering angle as long as $\theta \neq 0$. For any given steering angle θ of the PS-STLC, we derived an upper bound of SER of the uplink NOMA-IoT network. We validated the analytical results via extensive computer simulations. We leave the SER analysis when more than two sensors exist for further study.

REFERENCES

[1] L. Dal, B. Wang, Y. Yuan, S. Han, C. I, and Z. Wang, "Non-orthogonal multiple access for 5G: Solutions, challenges, opportunities, and future research trends," *IEEE Commun. Mag.*, vol. 53, no. 9, pp. 74–81, Sept. 2015

[2] Z. Ding, Y. Liu, J. Choi, Q. Sun, M. Elkashlan, C. I, and H. V. Poor, "Application of non-orthogonal multiple access in LTE and 5G networks," *IEEE Commun. Mag.*, vol. 55, no. 2, pp. 185–191, Feb. 2017

[3] Y. Chen, A. Bayesteh, Y. Wu, B. Ren, S. Kang, S. Sun, Q. Xiong, C. Qian, B. Yu, Z. Ding, S. Wang, S. Han, X. Hou, H. Lin, R. Visoz, and R. Razavi, "Toward the standardization of non-orthogonal multiple access for next generation wireless networks," *IEEE Commun. Mag.*, vol. 56, no. 3, pp. 19–27, Mar. 2018

[4] F. Kara and H. Kaya, "SER performances of downlink and uplink NOMA in the presence of SIC errors over fading channels," *IET Communications*, vol. 12, no. 14, pp. 1834–1844, Sept. 2018

[5] M. Al-Imari, P. Xiao, M. A. Imran, and R. Tafazolli, "Uplink non-orthogonal multiple access for 5G wireless networks, in *Proc. 11th Int. Symp. Wireless Commun. Syst. (ISWCS)*, Barcelona, Spain, Aug. 2014, pp. 781–785.

[6] J. S. Yeom, H. S. Jang, K. S. Ko, and B. C. Jung (2018), "BER performance of uplink NOMA with joint maximum likelihood detector, Manuscript submitted for publication.

[7] J. Joung, "Space-time line code," *IEEE Access*, vol. 6, pp. 1023–1041, Feb. 2018.

[8] J. Joung, "Spacetime line code for massive MIMO and multiuser systems with antenna allocation, *IEEE Access*, vol. 6, pp. 962–979, Feb. 2018.

[9] J. Joung, "Energy efficient spacetime line coded regenerative two-way relay under per-antenna power constraints, *IEEE Access*, pp. 47026–47035, Sept. 2018.

[10] J. Joung and E. -R. Jeong, "Multiuser spacetime line code with optimal and suboptimal power allocation methods, *IEEE Access*, vol. 6, pp. 51766–51775, Oct. 2018.

[11] J. Joung and B. C. Jung, "Machine learning based blind decoding for spacetime line code (STLC) systems, *IEEE Trans. Veh. Technol.*, vol. 68, no. 5, pp. 5154–5158, May 2019.

[12] D. Tse and P. Viswanath. *Fundamentals of wireless communication*, Cambridge University Press, 2005.